

Supporting Information

Hybrid Van der Waals Heterostructures of Zero-Dimensional and Two-Dimensional Materials

Zhikun Zheng^{*ab}, Xianghui Zhang^a, Christof Neumann^a, Daniel Emmrich^a, Andreas Winter^c,
Henning Vieker^{†a}, Wei Liu^d, Marga Lensen^c, Armin Götzhäuser^a and Andrey Turchanin^{*c}

Contents

1. Materials
2. Sample preparation
3. Characterization
4. Mechanical characterization of heterostructures by AFM bulge testing
5. Flipped-over NBPT nanomembrane
6. Flipped-over 1,1'-biphenyl-4-thiol (BPT) nanomembrane
 - 6.1. Formation of BPT nanomembrane.
 - 6.2. Preparation of self-assembled monolayers (SAMs) of 1H,1H,2H,2H-perfluorooctyl-trichlorosilane (PFOTS) on SiO₂/Si.
 - 6.3. Flipping BPT nanomembrane over.
 - 6.4. XPS analysis of flipped-over BPT nanomembrane on CF₃(CF₂)₅(CH₂)₂SiCl₃/SiO₂/Si.
7. Table S1
8. Figures S1-S4
9. Supporting references

1. Materials

4'-Nitro-1,1'-biphenyl-4-thiol (NBPT) (Taros, 95%) was purified by sublimation. N, N-dimethylformamide (DMF) was dried over 4 Å molecular sieves. Au NPs with a diameter of about 16 and 55 nm are synthesized by a standard sodium citrate reduction method. All other chemicals were used as received.

2. Sample preparation

Formation of JNMs: Mica substrates with 300 nm thermally evaporated Au (Georg Albert PVD) were cleaned in an UV/ozone cleaner (FHR), rinsed with ethanol, and blown dry by N₂. They were then immersed in 1 mmol L⁻¹ solution of NBPT in dry and degassed DMF for three days in a sealed flask under N₂. The samples were rinsed with DMF, ethanol, and dried in a N₂ stream. Crosslinking was performed in high vacuum ($< 5 \times 10^{-7}$ mbar) with an electron floodgun (Specs FG20) at energy of 100 eV and a dose of 60 mC cm⁻².

Functionalization of JNM: JNM-C₆₀/Au was prepared by immersing JNM/Au in 1 mM benzene solution of C₆₀ for 24 hours at room temperature. The resulting sample is thoroughly rinsed in benzene and dichloromethane to remove residual physisorbed C₆₀, followed by blowing dry with N₂. For the functionalization of the lower side of JNM-C₆₀, it was suspended at the surface of an aqueous solution of 40 mM PDDA (0.5 M NaCl) for 10 min, and successively suspended over the surface of as synthesized Au NPs solution for 30 min.

3. Characterization

X-Ray photoelectron spectroscopy (XPS) was carried out on Omicron ultra-high vacuum (UHV) spectrometer (base pressure below 10⁻¹⁰ mbar) with a monochromatic X-ray (Al K α) source. Binding energies are referred to the Au4f_{7/2} peak at 84.0 eV for the samples on gold, or to the main peak of the C1s signal at 284.2 eV for samples transferred onto SiO₂. Thickness calculations were based on attenuation of the substrate Au4f_{7/2} ($\lambda = 36$ Å) or Si2p ($\lambda = 35$ Å)

signals. For peak fitting, a Shirley background and symmetric Voigt functions were used. The separation between S2p_{3/2} and S2p_{1/2} was taken to be 1.2 eV.

Helium Ion Microscopy (HIM) was performed with a Carl Zeiss Orion Plus. The helium ion beam was operated at 35 - 36 kV acceleration voltage at a current of 0.5 - 1.5 pA. We used a 10 μm aperture at Spot Control 4 - 5. Secondary electrons were collected by an Everhart-Thornley detector at a 500 V grid voltage. The working distance was about 30 mm at a sample tilt of 35°. A dwell time per pixel of 0.5 - 1 μs with line averaging (Figure 4 b,c) or frame averaging (Figure 4a,e,f) was used. To compensate charge buildup, the electron flood gun was operated at 680 V in line mode.

Scanning Transmission Ion Microscopy (STIM) was performed at the HIM with a commercially available STIM stage. The sample is placed on a graphite block having at its center a cylindrical opening with a diameter of about 1 mm. Helium ions that are scattered hit the side walls of the graphite channel, while less- or non-scattered ions pass through the graphite opening. The graphite block is mounted over a polished metal plate facing towards the Everhart-Thornley detector. Ions passing the graphite channel generate SEs at the metal plate and these SEs are detected by the standard Everhart-Thornley detector. By scanning the focused ion beam over the sample, the SE signal from the metal plate forms the transmission signal. In order to prevent the thin membrane from rupturing due to charging, the electron flood gun was also used for charge compensation in this mode. The floodgun energy was set to 660 eV and was operated in line mode.

4. Mechanical characterization of heterostructures by AFM bulge testing

In the bulge test the pressure-deflection relation for a pressurized nanomembrane is given by

$$p = c_1 \frac{\sigma_0 t}{a^2} h + c_2 \frac{Et}{a^4(1-\nu)} h^3 \quad (1)$$

where the applied pressure p is a function of the deflection h at the center of the membrane.¹

Young's modulus E and prestress σ_0 could be determined from the pressure-deflection curve.

The pressure p is balanced both by the prestress σ_0 in the membrane, as expressed in the first linear term, and the strain energy of the membrane, as expressed in the second cubic term. The thickness t of the membrane is calculated from X-ray photoelectron spectroscopy (XPS) measurements, as shown in table S1. Since JNMs are similar to polymers with a typical Poisson's ratio in the range of 0.3-0.4, here we employed a Poisson's ratio of 0.35 for the calculations. The parameters c_1 and c_2 depend on the initial displacement field of the membrane and they are the function of membrane aspect ratio; both values (c_1 and c_2) were calculated numerically based on the energy minimization method.

To provide a model estimation of the mechanical properties of the heterostructures, a formula according to the mixture law was used.² Note that JNM/(C₆₀-JNM)_n are multilayer films consisting of JNM and (C₆₀-JNM)_n layers. The Young's modulus of such multilayer system can be estimated as

$$E_{\text{heterostructure}} = \frac{t_{JNM}}{t_{\text{heterostructure}}} E_{JNM} + n \frac{t_{C_{60}-JNM}}{t_{\text{heterostructure}}} E_{C_{60}-JNM} \quad (2)$$

where $E_{\text{heterostructure}}$, E_{JNM} and $E_{C_{60}-JNM}$, and $t_{\text{heterostructure}}$, t_{JNM} and $t_{C_{60}-JNM}$ represent the Young's modulus and effective thickness of the heterostructures, the JNM and the single layer C₆₀-JNM, respectively. All experimental data agree well with results of the obtained by this formula (see Table S1).

5. Flipped-over NBPT nanomembrane

Here we present a procedure to flip over a JNM and to transfer it onto a new substrate where the originally bottom S-side becomes to be the terminal one. Figure S3 shows a scheme of this procedure. First, a JNM/Au is detached from mica by HF etching. After washing with water, it is placed into acetone, flipped-over and transferred onto a new target substrate, e.g., an oxidized Si wafer as employed here. Acetone has a lower surface tension in comparison to water and it wets the JNM, the gold layer and the target substrate protects the JNM and makes the flip-over procedure possible. Then, the remaining gold layer is etched in an I₂/KI bath leaving a JNM with the S-side on top. We analyzed the flipped over JNMs by XPS (Figure S4). To prove, that the S-side forms now the terminal surface of the JNM we applied angle resolved XPS (ARXPS) measurements, Figure S3b and S3c. The surface sensitivity of XP signals increases with an increasing emission angle for photoelectrons, θ , so the layered structure of the JNM can be revealed by intensity changes of the S2p, C1s and N1s signals with θ .³ As seen from Figure S3b, JNM on the original gold substrate, an increase in the intensity of the N1s signal is high with increasing θ followed by the intensities of the C1s and S2p signals, whereas for the flipped over JNM this sequence is inverted. These angular dependencies clearly demonstrate that the S-side of the flipped over JNM forms the terminal surface, whereas for the JNM on the original substrate the N-side is terminal. The developed flip-over procedure was also successfully applied for nanomembranes made of other molecular precursors (Figure S5) and can be generally adapted to a variety of free-standing 2D materials.

6. Flipped-over 1,1'-biphenyl-4-thiol (BPT) nanomembrane

6.1. Formation of BPT nanomembrane. Mica substrates with 300 nm thermally evaporated Au (Georg Albert PVD) were cleaned in an UV/ozone cleaner (FHR), rinsed with ethanol, and blown dry in N₂. They were then immersed in circa 1 mmol L⁻¹ solution of BPT (Platte Valley Scientific) in dry and degassed DMF for three days in a sealed flask under N₂. The samples were rinsed with DMF, ethanol, and dried in a N₂ stream. Cross-linking was performed in high vacuum ($< 5 \times 10^{-7}$ mbar) with an electron floodgun (Specs FG20) at energy of 100 eV and a dose of 60 mC cm⁻².

6.2. Preparation of self-assembled monolayers (SAMs) of 1H,1H,2H,2H-perfluorooctyl-trichlorosilane (PFOTS) on SiO₂/Si. The growth of SAMs of PFOTS (CF₃(CF₂)₅(CH₂)₂SiCl₃) on SiO₂/Si was done by vapor phase deposition.⁴ The SiO₂/Si substrates were placed on a sample holder in a desiccator. 10 μL of PFOTS was then placed in a dish in the desiccator. The dish was covered by a half open beaker as splashguard. The desiccator was sealed and connected to a vacuum pump. The samples are ready for further experiments after 2 hours pumping.

6.3. Flipping BPT nanomembrane over. BPT nanomembrane was flipped over with the same procedure as that developed for JNM as described above. Different substrates were used as the supporting media for the flipped-over JNM and BPT nanomembrane since appropriate membrane-substrate interactions help keep the membrane intact during all the transfer and cleaning procedures. SiO₂/Si has a slightly negative charge and it has hydroxyl groups on its surface, which can adsorb the amino side of the flipped-over JNM by either electrostatic interaction or hydrogen bond formation. CF₃(CF₂)₅(CH₂)₂SiCl₃/SiO₂/Si has a strongly hydrophobic surface, which can adsorb the benzene ring side of the flipped-over BPT membrane by hydrophobic interactions.

6.4. XPS data analysis of flipped-over BPT membrane on $\text{CF}_3(\text{CF}_2)_5(\text{CH}_2)_2\text{SiCl}_3/\text{SiO}_2/\text{Si}$. The chemical composition and structure of the flipped-over BPT nanomembrane on $\text{CF}_3(\text{CF}_2)_5(\text{CH}_2)_2\text{SiCl}_3/\text{SiO}_2/\text{Si}$ were characterized by XPS. The total intensity of the S2p signals was the same as that of BPT nanomembrane on Au/mica, which indicated a successful transfer. Due to the presence of diverse chemical species (CF_3^- , CF_2^- , CH_2^- , etc.), the C1s signal consists of several XP peaks. The main species are marked in Figure S5a. To prove BPT nanomembrane was flipped-over and S-side is now the terminal surface, angle-resolved XPS (ARXPS) was performed. The surface sensitivity of the XP signals increases with increasing emission angle of the photoelectrons, θ (Figure S5b), so the layered structure of the nanomembrane can be revealed by the ARXPS of the S2p, C1s-BPT, C1s- CF_2 , and C1s- CF_3 signals. As seen from Figure S4b, an increase in the intensity of the S2p signal is high with increasing θ followed by the intensities of the C1s-BPT, C1s- CF_2 , and C1s- CF_3 signals. These angular dependencies clearly demonstrate that the BPT nanomembrane is flipped over on $\text{CF}_3(\text{CF}_2)_5(\text{CH}_2)_2\text{SiCl}_3/\text{SiO}_2/\text{Si}$.

7. Table S1

Table S1. Thickness and experimental and calculated Young's moduli

| Membranes | Thickness [Å] | Experimental Young's modulus [GPa] | Calculated Young's modulus [GPa] |
|---|------------------|---------------------------------------|-------------------------------------|
| JNM | 11 | 9.0±1.5 | n/a |
| C ₆₀ -JNM | 17 | 6.8±1.5 | n/a |
| JNM/(C ₆₀ -JNM) ₁ | 28 | 7.5±1.8 | 7.7 |
| JNM/(C ₆₀ -JNM) ₂ | 44 | 7.2±1.3 | 7.4 |
| JNM/(C ₆₀ -JNM) ₃ | 60 | 8.7±1.5 | 7.2 |

8. Figures S1-S5

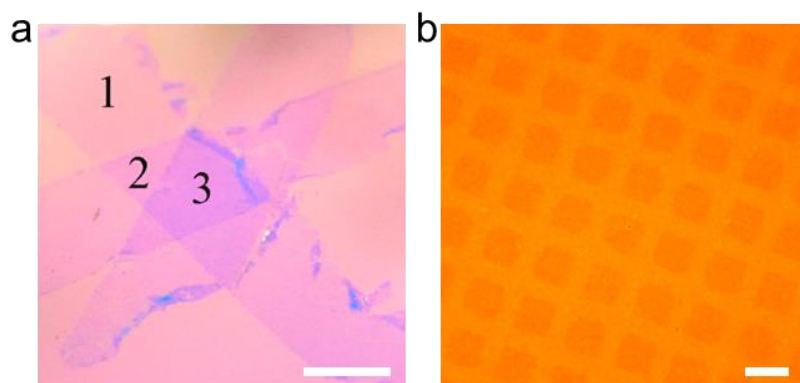


Figure S1. Lithography of C₆₀-JNM hybrid heterostructures. a) Photographic image of patterned C₆₀-JNMs on 285 nm SiO₂/Si. The number of sheets is indicated. The heterostructure was assembled scissor cutting of parallel stripes of C₆₀-JNMs and stacking them by roughly 60° relative to each other. b) Optical microscopy image of patterned C₆₀-JNMs on polycrystalline Au substrate. The scale bars in a) and b) are 0.5 cm, and 40 μm, respectively.

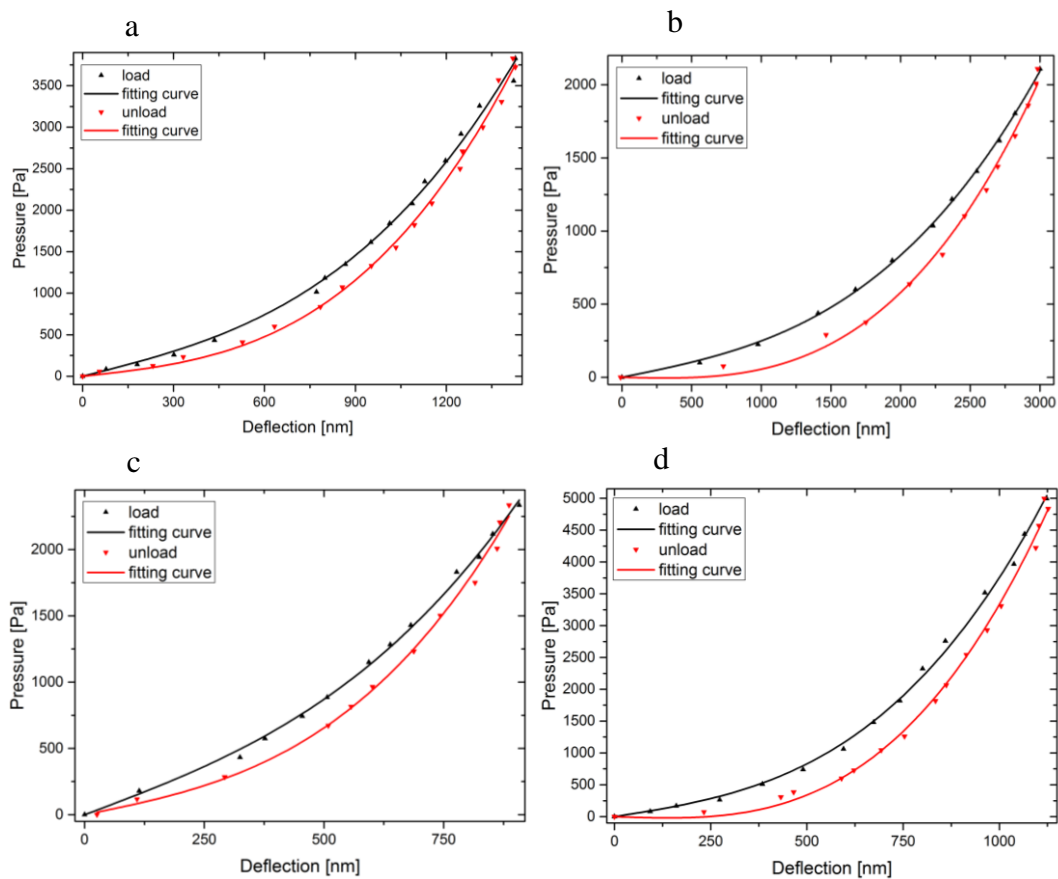


Figure S2. Pressure-deflection curves of a) a JNM, b) a C_{60} -JNM, c) a JNM/ $(C_{60}$ -JNM)₁ membrane and d) a JNM/ $(C_{60}$ -JNM)₃ membrane.

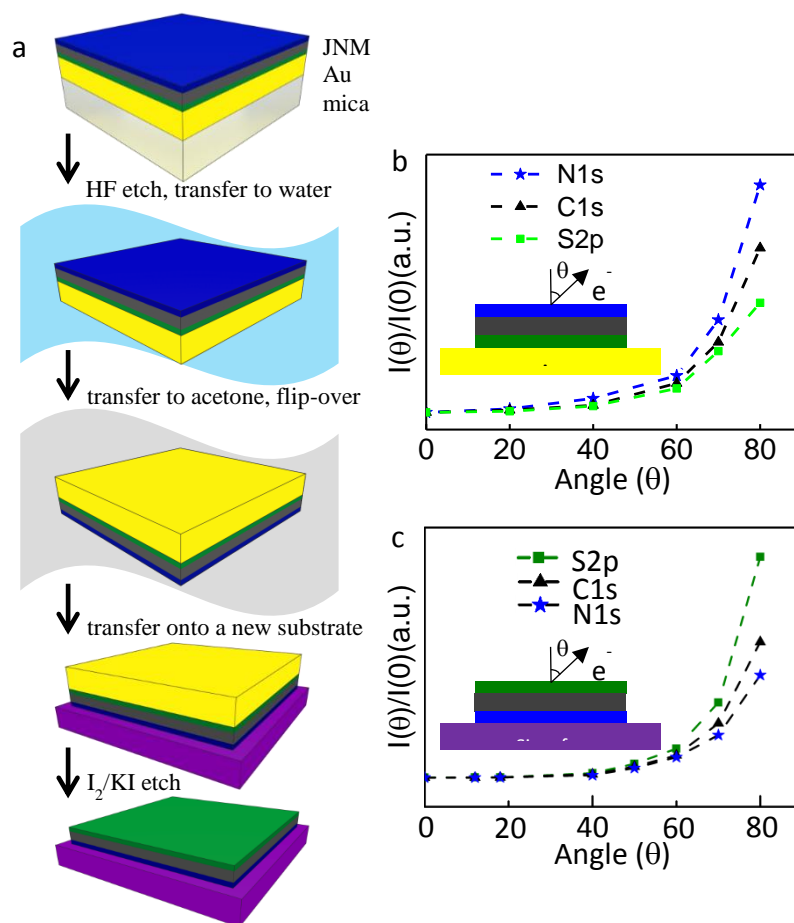


Figure S3. Flipped-over JNMs. a) Schematic of the experimental procedure, see text for details. Color code: blue, black and green are N, C and S spices of the JNM, respectively; yellow, Au; light grey, mica; light blue, water; light green, acetone; purple, arbitrary substrate. Angle resolved XPS data a JNM on gold, b), and of a flipped-over JNM on a Si-wafer, c). Relative intensities, $I(\theta)/I(0^\circ)$, of the S2p (green), C1s (black) and N1s (blue) signals are presented as a function of the photoelectron emission angle, θ (see insets).

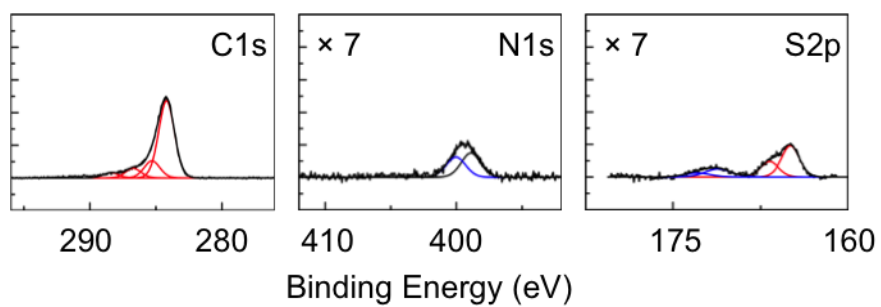


Figure S4. C1s, N1s and S2p of a flipped-over NBPT membrane on 285 nm SiO₂/Si substrate.

The S2p and N1s spectra were expanded by a factor of 7.

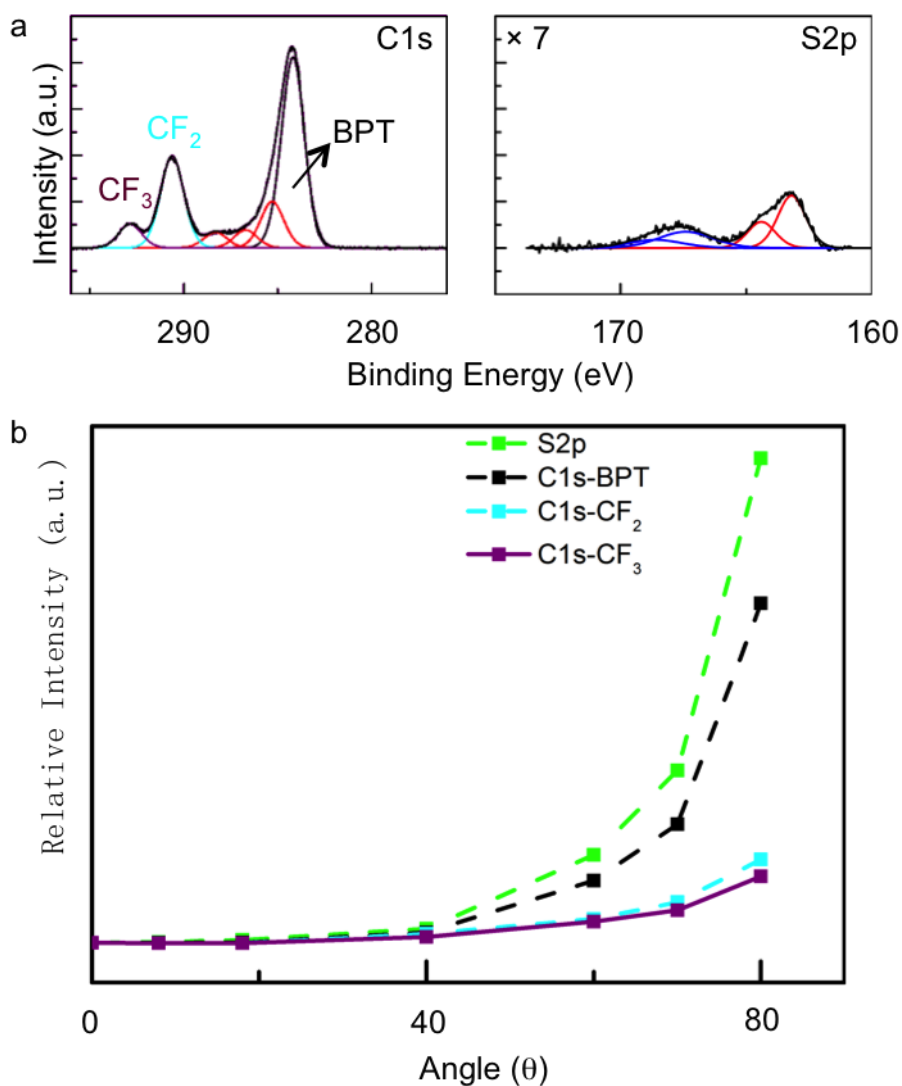


Figure S5: a) XPS of a flipped BPT membrane on 285 nm SiO_2/Si . XPS of a flipped-over BPT membrane on $\text{CF}_3(\text{CF}_2)_5(\text{CH}_2)_2\text{SiCl}_3/\text{SiO}_2/\text{Si}$. The S2p spectrum was expanded by a factor of 7. b) Relative signal intensities of S_{2p} (green), C_{BPT} (black), $\text{C}_{1s-\text{CF}_2}$ (cyan) and $\text{C}_{1s-\text{CF}_3}$ (purple) of the flipped membrane as a function of the emission angle.

9. Supporting references

[1] a) J. J. Vlassak, W. D. Nix, *J. Mater. Res.* 1992, 7, 3242; b) X. H. Zhang, A. Beyer, A. Götzhäuser, *Beilstein J. Nanotechnol.* **2011**, 2, 826.

[2] a) O. R. Shojaei, A. Karimi, *Thin Solid Films* 1998, 332, 202; b) P. Martins, P. Delobelle, C. Malhaire, S. Brida, D. Barbier, *Eur. Phys. J. Appl. Phys.* **2009**, 45, 10501.

[3] C. Nottbohm, A. Turchanin, A. Götzhäuser, *Z. Phys. Chem.* **2008**, 222, 917.

[4] G. Y. Jung, Z. Y. Li, W. Wu, Y. Chen, D. L. Olynick, S. Y. Wang, W. M. Tong, R. S. Williams, *Langmuir* **2005**, 21, 1158.